

# PROCEEDINGS OF SPIE

[SPIDigitalLibrary.org/conference-proceedings-of-spie](https://SPIDigitalLibrary.org/conference-proceedings-of-spie)

## UV capabilities of the CETUS multi-object spectrometer (MOS) and NUV/FUV camera

Stephen E. Kendrick, Robert A. Woodruff, Tony Hull, Sara R. Heap, Alexander Kuttyrev, et al.

Stephen E. Kendrick, Robert A. Woodruff, Tony Hull, Sara R. Heap, Alexander Kuttyrev, William Danchi, Lloyd Purves, "UV capabilities of the CETUS multi-object spectrometer (MOS) and NUV/FUV camera," Proc. SPIE 10699, Space Telescopes and Instrumentation 2018: Ultraviolet to Gamma Ray, 1069939 (6 July 2018); doi: 10.1117/12.2314114

**SPIE.**

Event: SPIE Astronomical Telescopes + Instrumentation, 2018, Austin, Texas, United States

# UV capabilities of the CETUS multi-object spectrometer (MOS) and NUV/FUV camera

Stephen E. Kendrick<sup>\*a</sup>, Robert A. Woodruff<sup>b</sup>, Tony Hull<sup>a,c</sup>, Sara R. Heap<sup>d</sup>, Alexander Kutyrév<sup>e</sup>, William Danchi<sup>f</sup>, Lloyd Purves<sup>f</sup>

<sup>a</sup>Kendrick Aerospace Consulting LLC, Lafayette, CO, USA

<sup>b</sup>Woodruff Consulting, Boulder, CO, USA

<sup>c</sup>University of New Mexico, Albuquerque, NM, USA

<sup>d</sup>NASA GSFC emerita, Greenbelt, MD, USA

<sup>e</sup>University of Maryland, College Park, MD, USA

<sup>f</sup>NASA GSFC, Greenbelt, MD, USA

## ABSTRACT

The Cosmic Evolution Through UV Spectroscopy (CETUS) concept<sup>1-3</sup> enables parallel observations by the UV multi-object spectrometer (MOS) and near-UV/far-UV camera which operate simultaneously but independently with their separate field of views.

The near-UV MOS can target up to 100 objects at a time without confusion with nearby sources or background zodiacal light. This multiplexing will allow over 100,000 galaxies to be observed over a typical mission lifetime. The MOS includes a next-generation micro-shutter array (NGMSA), an efficient aspheric Offner-like spectrometer design with a convex grating, and nanotube light traps for suppressing unwanted wavelengths. The NUV/FUV Camera has the capability to image in a range of sub-bands from 115-400 nm at the same time the MOS is operating at 180-350 nm. The UV camera has a similar Offner-like relay, selectable filters, and two separate detectors to optimize observing in either the far-UV (115-175 nm) or the near-UV (180-400 nm) utilizing a CsI Micro-Channel Plate detector (MCP) and a CCD respectively.

**Key words:** ultraviolet, spectrometer, camera, micro-shutter array, nanotubes

## 1. OVERVIEW

The 2010 Astrophysics Decadal Survey panel recommended a full-scale study of galaxies at redshifts,  $z \sim 1-3$ , as a follow-up to the imaging and spectroscopic survey of the Sloan Digital Sky Survey (SDSS). The CETUS camera and multi-object spectrograph are poised for such observations.

A near UV multi-object spectrograph is proposed as one of the three major instruments of the 1.5-m aperture CETUS probe mission concept. The UV MOS is designed to efficiently observe 50-100 galaxies at a time to build-up a near-UV spectral survey of  $10^5$  galaxies at  $z=1-2$ . The spectrograph will be a slit MOS in order to prevent confusion with nearby sources and to block unwanted background like zodiacal light. A next generation micro-shutter array (MSA) provides a readily configurable array of slits. **Figure 1** shows an example of an MSA MOS approach to spectroscopic investigations. The strongest and most important diagnostic spectral features fall in the rest-frame far-UV ( $\sim 100-200$  nm), which Hubble spectrographs have exploited to study low-redshift galaxies. At redshift,  $z \sim 1$ , these far-UV spectral features are redshifted into near-UV ( $\sim 200-400$  nm). To optimize the throughput in the UV, the number of reflections must be minimized, so

---

\* SKconsulting@comcast.net

there are no fold mirrors in the instrument. An Offner-based magnification one-to-one imaging approach provides a wide field of view enabling low the survey to be taken more quickly and incorporates a convex grating for dispersion.

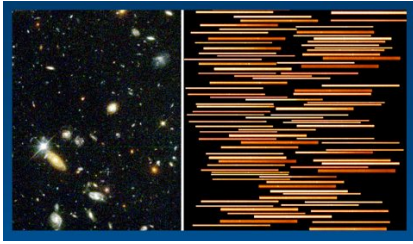


**Figure 1**-- Example of Multi-Object Spectrograph concept applied to studying multiple galaxies simultaneously<sup>4</sup>. The left panel shows galaxies in the FoV of the MOS while the right panel shows the spectra of the galaxies chosen for study by appropriate configuration of the micro-shutter array.

Straylight and out-of-band radiation is a concern, so the MOS is designed for the 200 nm – 350 nm desired band to be in reflection and the unwanted wavelengths transmitted to nanotube beam dumps in key areas. The optical coatings on the mirrors are designed to optimally reflect the 180 nm – 350 nm light and conversely transmit or absorb the longer wavelengths that we do not want to reach the science detector.

The NUV/FUV camera similarly has an Offner-like relay which feeds either a NUV channel (180-400 nm) with a 4Kx4K CCD or a FUV channel (115-180 nm) with a Micro-Channel Plate detector.

The Camera and the MOS can operate simultaneously or as standalone instruments. **Figure 2** shows one potential layout for these two instruments. As seen in **Figure 3**, the camera observes a region offset from the MOS.

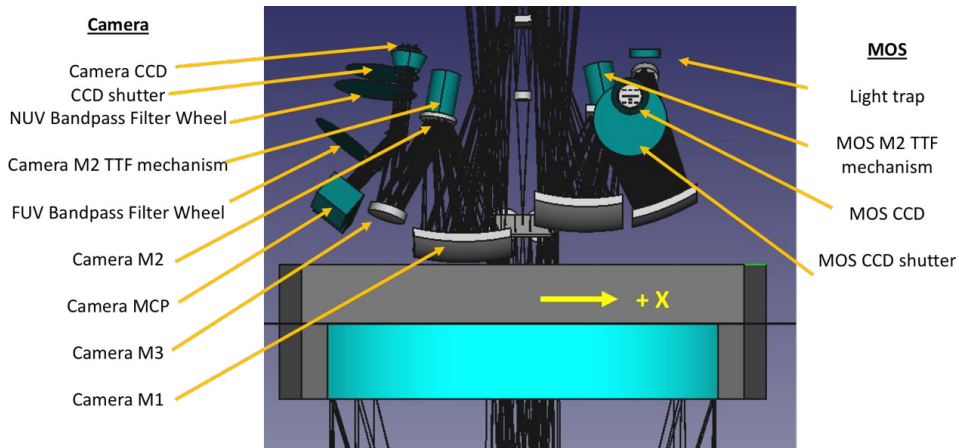


**Figure 2** -- The FUV/NUV Camera and MOS have similar relay optics from the CETUS optical telescope assembly and can be operated simultaneously. The two instruments can be independently installed and aligned to the telescope without interference -- allowing flexibility in the manufacturing and test schedule.

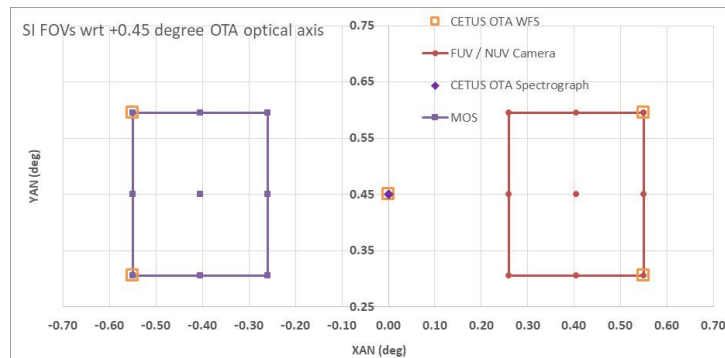


**Figure 3** – CETUS has a large FOV which is populated with 3 science instruments as well as fine guidance and wavefront sensors. The large FOV on the left (purple) is the MOS and the FUV/NUV Camera FOV is on the right (red).

## 2. DERIVED CETUS TELESCOPE AND INSTRUMENT REQUIREMENTS

**Telescope:** Requirements for the CETUS telescope<sup>5</sup> are derived from the science objectives described briefly in Section 1 and more thoroughly in our study of  $z=1-2$  galaxies. The objective is to make a massive near-UV spectroscopic survey of  $z=1-2$  galaxies to uncover their physical properties and processes operating in them. To make such a survey, the telescope must have the light-gathering power of a 1.5-m telescope to reach galaxies with near-UV fluxes as low as  $4 \times 10^{-18}$  erg/s/cm<sup>2</sup>/Å plus wide field coverage enabled by a  $f/5$  telescope.

**UV Multi-Object Spectrograph:** The requirements for the spectrograph (Table 1) are derived from the goals and requirements of a UV MOS as described in the Cosmic Origin Program Annual Technology Report (PATR<sup>6</sup>) as well as our study of  $z=1-2$  galaxies. The study must involve a massive spectral survey of  $z=1-2$  galaxies. As explained by Gunn<sup>7</sup>, only with a large survey can we make a statistically significant separation of processes driving galaxy evolution at  $z \sim 1-2$ . “A survey must be large ( $\sim 10^5$  galaxies) in order to disentangle covariances in the physical properties of galaxies... Accurate measurement of the correlation function typically requires samples of  $10^4$  galaxies or more.” A practical problem then arises: galaxies at  $z=1$  are only 0.5% as bright as at  $z=0.1$ , and galaxies at  $z=2$  are fainter still, so a survey of such galaxies is out of Hubble’s reach, which has to acquire spectra of galaxies one by one. But a Probe-class mission having a wide-field, 1.5-m telescope and near UV multi-object spectrograph (MOS)<sup>8-10</sup> observing 50-100 galaxies at a time *can* make a near-UV spectral survey of  $10^5$  galaxies at  $z=1-2$  in less than 5 years.

The field of view of the MOS is  $1045'' \times 1045''$ . It contains  $\sim 100$   $z=1-2$  galaxies meeting the flux requirement above. The MOS uses a micro-shutter array (MSA)<sup>11</sup> with selectable slits to eliminate confusion with nearby sources and to block unwanted background. Our study showed that the half-light diameters of  $z=0.8-1.3$  galaxies range from  $0.2''$  to  $2''$ , with a median at  $0.9''$ . Each shutter subtends  $2.75'' \times 5.50''$ , which encompasses nearly all of a galaxy at  $z \sim 1$ . Nevertheless, some of the  $\sim 100$   $z=1-2$  galaxies will not be selected for spectroscopy, because they land at the edge of a shutter, but at least half should be well situated in a shutter.

**Table 1** Derived MOS Requirements

Parameter	MOS Requirement
Wavelength range	180 – 350 nm
Wavelength resolution	2 to 4 Angstroms (1 pixel)
Sampling	Nyquist sampling or better
Substepping	$1/4^{\text{th}}$ pixel per step
Substepping range (for dithering)	4 pixels
Field of View (FOV)	$1045'' \times 1045''$
Spatial resolution	1 pixel ( $0.33''$ )

size ( $12$  microns  $\rightarrow 0.33''$ ). The makers of the CCD (e2v) will use special coatings to boost the QE in the near-UV band). Because the CCD is also sensitive to wavelengths longer than  $350$  nm (which would be a source of background noise to our UV instrument), the MOS contains dichroic coatings on the dichroic beamsplitter filter and the two Offner mirrors, M1 and M3, to direct longer wavelengths into light traps which are coated with carbon nanotubes.

**NUV/FUV Camera:** The CETUS camera is required for proper analysis and interpretation of the MOS spectra and for independent studies. CETUS camera images will have a resolution 10 times finer than GALEX images and will enable morphological studies of large galaxies. Combined with images to be obtained by large telescopes such as Subaru’s Hyper-Suprime Cam, it will enable direct localization of star-formation in galaxies of redshifts,  $z=0$  to  $2$ . The requirements for the CETUS Camera are shown in Table 2.

The spectral range of the MOS is  $180-350$  nm. The spectral resolving power,  $R \sim 1000$ , is adequate to yield line profiles of important spectral features like stellar wind lines. This resolving power corresponds to a 1-pixel resolution with Nyquist sampling accomplished by slight shifts of the detector in the direction of dispersion.

The optical efficiency of the three optics in the Offner spectrograph is  $\sim 65\%$ . The design efficiency of the convex grating is expected to be  $>60\%$  at the blaze wavelength ( $250$  nm). We have adopted a UV-sensitive CCD similar to the CCD in the Euclid because it has been space-qualified, and its pixel

**Table 2** Derived NUV/FUV Camera Requirements

Parameter	FUV Requirement	NUV Requirement
Wavelength range	115 – 175 nm	180 – 400 nm
Spatial resolution	$< 550$ mas FWHM	$< 410$ mas FWHM
Sampling	10 microns	Nyquist or better
Dithering range	$>10$ pixels (TBD)	$>10$ pixels (TBD)
Field of View (FOV)	$1045'' \times 1045''$	$1045'' \times 1045''$
Pixel width	20 microns	12 microns

### 3. CRITICAL TECHNOLOGIES FOR A SUCCESSFUL UV MOS AND NIR/FUV CAMERA

The critical technologies for the UV MOS and the NUV/FUV Camera are listed in **Table 3**. The NGMSA is the key technology for further development and that is proceeding at GSFC.

**Table 3** The pertinent UV MOS and NUV/FUV Camera optical technologies are mature or will be advanced to meet CETUS schedule requirements

Technology	Heritage/ Comments
Alignment of aspheric Offner Camera	Comparable aspheric systems have been previously aligned. Arizona Optical Systems (AOS) and others have proven proprietary methods to align Offner mirrors and the convex grating
High UV-reflectivity dichroic beamsplitter filter	FUV/NUV dichroic beam splitter on GALEX. Similar dichroic coatings have been demonstrated on small samples (MacKenty 2016) by Materion
High UV-reflectivity coatings on Offner mirrors	Materion (Barr) and ZeCoat are proficient in making special multi-layer UV coatings at these wavelengths
Red leak suppression using light trap for dichroic beamsplitter	Carbon nanotube technology has proven effective in a NASA laboratory. Painting the backs of M1 and M3 mirrors is also a consideration.
Next-Generation Micro-Shutter array	Success of APRA 2015 program; Separate SAT 2016 proposal to advance TRL of the NG-MSA (Mary Li, PI), and also a SAT 2017 that has been proposed (Greenhouse, PI)
Convex Grating	Convex gratings have been used for Hyperspectral imaging, but not yet in UV. Zeiss has experience making convex gratings.
Sub-stepping and dithering capability	Sub-stepping is common on all Hubble spectrographs. Sub-stepping and dithering (large steps) will be carried out by the same mechanism installed on the Camera M2 mirror and the MOS M2 grating.
Micro channel Plate (MCP) detector with high quantum efficiency in the FUV	The CETUS far-UV detector made by U.C. Berkeley Space Science Lab is the same as on the Hubble COS spectrograph.
All elements work together as an instrument system	Plan for integration of scientific instruments allow for different suppliers and schedules of the MOS and Camera

### 4. DETAILED MOS DESIGN

#### 4.1 Detailed Optical Design

We have developed an Offner-like spectrograph<sup>12,13</sup> operating over a wavelength range of 180 – 350 nm. The system operates at  $f/5$  and has unit magnification. The dispersion from the grating gives 0.2 to 0.4 nm/pixel or 1-pixel resolution of 1000 for 12  $\mu\text{m}$  pixels. Coupled with a 1.5-m telescope design, the system EFL is 8.3 m which gives a plate scale of 0.37 arcsec/pixel for 12  $\mu\text{m}$  pixels. The field of view is 1045 x 1045 arcsec.

A block diagram of the optical design is shown in **Figure 4** and a functional view shown in **Figure 5**. **Figure 6** shows the current optical design. The system is 800 mm long, 450 mm wide and 230 mm tall (out of plane). The field of view shown assumes a 38 mm x 38 mm source defined by the size of the micro-shutter array.

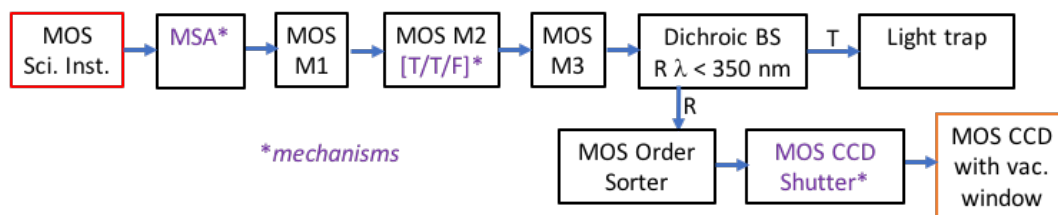


**Figure 4** -- MOS Functional Block Diagram showing the optical path sequence and major functions

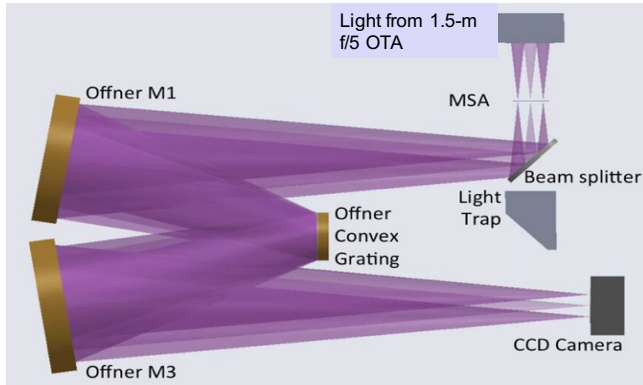


**Figure 5** – The number of surfaces is minimized for high UV throughput while the aspheric design offers excellent image quality

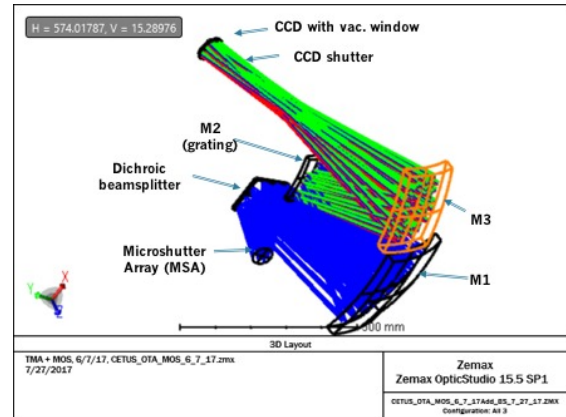


**Figure 6** – Several layout trades are in process as the 3 instruments of CETUS are being packaged. This is the current MOS design layout.

The performance is shown shown in **Figure 7**

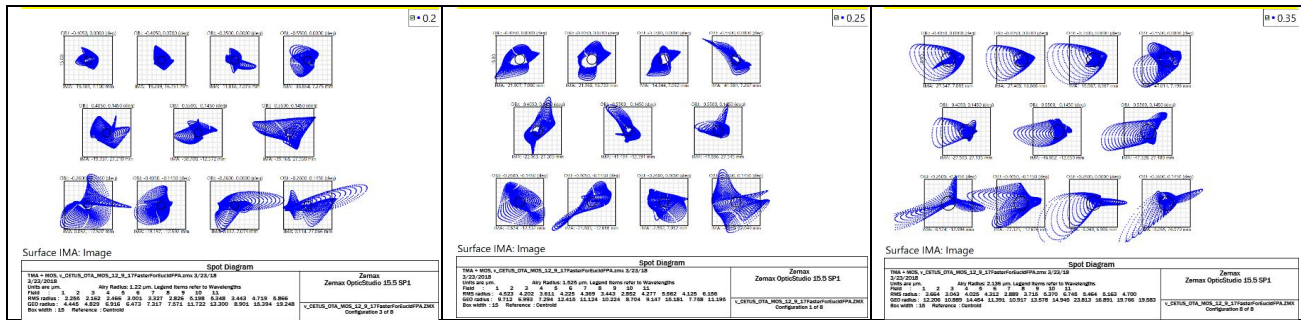


**Figure 7.a** -- Image at MOS CCD at 200 nm (boxes are 15  $\mu\text{m}$ ) including impact of 1.5-m aperture telescope

**Figure 7.b** -- Image at MOS CCD at 250 nm

**Figure 7.c** -- Image at MOS CCD at 350 nm

## 4.2 Optical Coatings, Straylight, and Contamination Control

The dielectric optical coatings for the MOS optics will be designed to reflect the in-band UV and transmit the longer wavelengths. This is a narrower band than the coatings on the 1.5-m aperture optical telescope assembly which feeds 3 instruments and two fine guidance sensors (which require a broader bandwidth). The design is based on coatings previously demonstrated by Materion<sup>14</sup> on small samples. The cut-off wavelength will be optimized for 350 nm rather than the 320 nm shown in **Figure 8**. The long wave cutoff can be shifted as desired.

Exceptional stray light control of out of band radiation can be accomplished by directing the light to a highly absorptive light trap comprised of carbon nanotubes<sup>15-17</sup>. Carbon nanotubes are extremely dark due to their electronic structure and vanishingly low density. Carbon in its bulk form has an index as high as 4 resulting in a strong reflectance; by tailoring the nanotube growth process, the fill factor of carbon can be reduced to less than one percent creating an effective index approaching unity. The light therefore sees no impedance mismatch. A carbon nanotube forest only 25 microns tall will strongly absorb light from the UV (only 0.87% to 0.52% reflectance) to the far infrared (<0.2% reflectance).

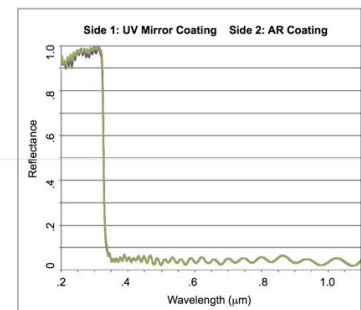


**Figure 8** – The coatings are designed to sharply reduce reflectance of light longer than 320nm. [Reflectance data adapted from Ref. 9]

**Figure 9** shows the hemispherical reflectance of carbon nanotubes grown on a metal substrate; compared to the ~ 4% reflectance of Z306 paint often used by NASA for stray light control. Hemispherical reflectance quantifies the total amount of light that is scattered by light striking a sample that is collected over a hemisphere. Measurements of the materials bi-directional reflectance function (BRDF) also indicate very low reflectance at glancing angles making this the ideal material for a light trap. The implementation of the light trap behind a dichroic beamsplitter in the micro-shutter path will greatly reduce out-of-band stray light in the system. Depending on the final design of the system, additional measures may be required to reduce stray light from the structure that holds the dichroic or within the Offner relay assembly.

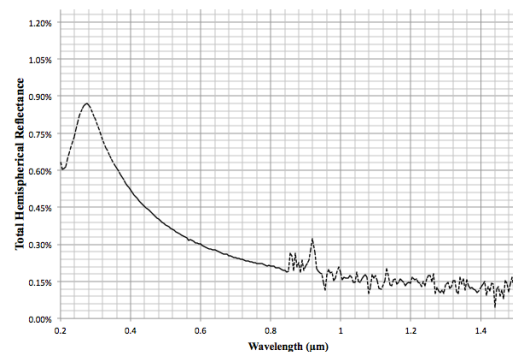


**Figure 9**– A nanotube light trap behind the beamsplitter will greatly reduce out-of-band scatter.

### 4.3 Next-Generation Micro-Shutter Array (NG-MSA)

The Micro-shutter Array (MSA) planned for MOS is based on the prior work done by Goddard Space Flight Center for the JWST NIRSpec instrument. However, the implementation has evolved as the Goddard team of scientists and engineers have continued to develop the micro-shutter array technology<sup>18</sup>. The size of each individual shutter is 100 μm x 200 μm. Compared to the MSA in JWST’s NIRSpec spectrograph, the NG-MSA will have 100 times faster actuation of the shutters, the possibility of large-format mosaics to cover a >50 times larger field of view, greater robustness with fewer mechanical failures, and a lower operational duty cycle on individual shutters.

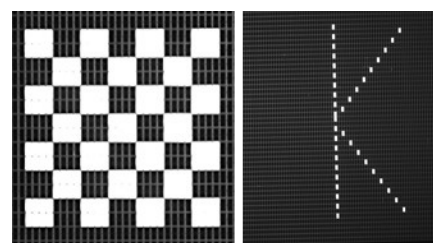


**Figure 10** -- 2-D addressing images from a 128x64 NGMSA array<sup>18</sup>

NG-MSAs are electrostatically actuated MEMS devices that can be used as multi-object selectors and filters in spaceborne applications. After the group at GSFC successfully built micro-shutter assemblies for JWST, they began working on the NGMSA development (starting in 2009) to incorporate operational simplifications and higher reliability. The NG-MSA has a simplified scalable design and is fully electrically actuated (unlike the JWST micro-shutters which require magnetic actuation). In addition, only the shutters to be opened have to be actuated so their duty cycle is lower than the earlier generation MSAs which significantly reduces the number of actuations per shutter, thus extending the lifetime and reducing the risk of failure.

GSFC has demonstrated 128x64 full array actuation and 2-D addressing on a fully integrated NG-MSA assembly, which brings the technology to TRL 4. Sample 2-D addressing images captured from a 128x64 NG-MSA array are shown in **Figure 10**. **Figure 11** depicts a MSA packaged assembly. The NG-MSA assembly for the CETUS UV MOS will nominally consist of a 380x190 NGMSA array with the shutter pixel size of 100μm x 200 μm, four IC drivers, over a hundred passive electronic components, and a PC board, similar to the assembly shown in **Figure 12**.

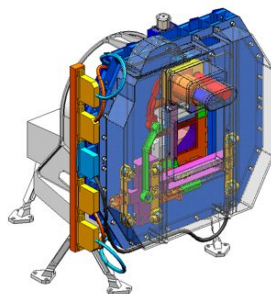


**Figure 11**-- JWST NIRSpec Micro-Shutter array Assembly (MSA) included four arrays of 365x170 shutters<sup>19</sup>.



**Figure 12** – An integrated NG MSA will be procured from GSFC using their existing facilities. A pilot design array with 128x64 shutters on a PC board with integrated drivers has been fabricated.

Work will continue in this area as the NGMSA is the assembly with the lowest TRL at this point. Several efforts are ongoing.

#### 4.4 Holographic Convex Grating

We have paid special attention to the grating, as it is the heart of the UV MOS. We are considering both Zeiss and Horiba to fabricate a holographic convex grating (140 lines/mm; RoC of 400 mm) with a blaze angle to increase efficiency at 250 nm. A fused silica substrate (e.g., Suprasil®) with an aluminum or enhanced coating is planned. The grating is expected to have a diffraction efficiency as high as 70% with a conservative example having a peak efficiency of ~50% shown in **Figure 13**. Like the first-order gratings in Hubble’s Goddard High Resolution Spectrograph (GHRS) and Cosmic Origins Spectrograph (COS), the grating is a holographic grating, which promises to produce very low scattered light. We will test for evidence of grating scatter using a D<sub>2</sub> continuum source and absorption cell filled with O<sub>3</sub>, which produces a sharp cut-off in flux at ~300 nm.

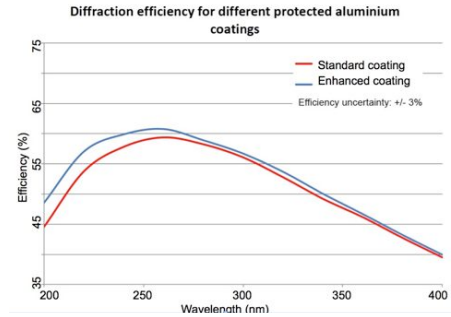


**Figure 13** -- Predicted grating efficiency for two different coatings [Zeiss]. We have selected the enhanced coating.

Any residual light below the 300-nm edge is most likely due to grating scatter. Similarly, the ratio of strengths of SO<sub>2</sub> absorption lines in a multiplet can be used to derive grating scatter. Comparison to their theoretical values will be an indication of the extent we have been able to control a) grating scatter, b) red light leak, c) MOS scattered light, d) optics scattered light, and e) scattered light from glints and contamination.

#### 4.5 CCD Detector

We are baselining identical 4K x 4K CCDs with 12 μm pixels for both the UV MOS and the NUV Camera channel. The e2v CCD 273-84 has been selected and has been qualified for launch on the Euclid mission. A shutter in front of the CCD controls the exposure time. **Figure 14** shows the device packaged for Euclid and **Figure 15** shows the accompanying SIDECAR ASIC. **Figure 16** shows the anticipated quantum efficiency over the 180-400 nm spectral band.

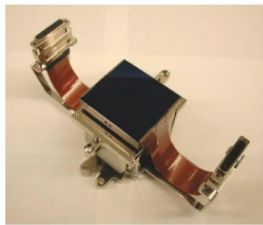


**Figure 14** -- e2v CCD 273-84 4K x 4K Focal Plane Array (12 micron pixel)

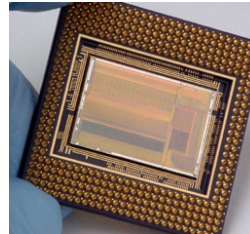


**Figure 15** -- The SIDECAR™ ASIC provides the ability to control the CCD including the ability to select “windows” for readout

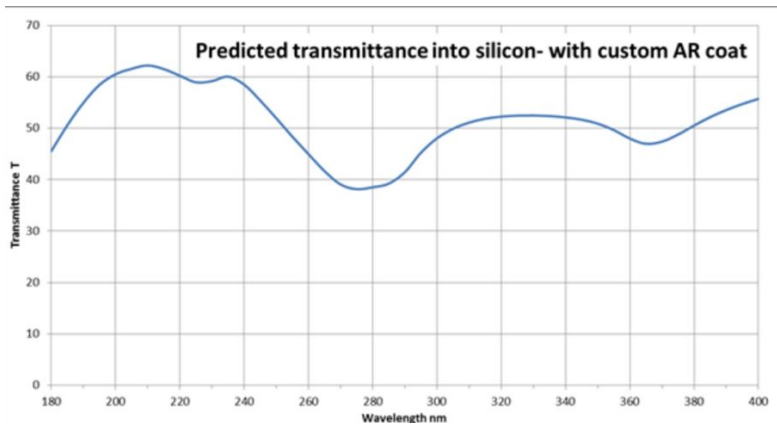


**Figure 16** -- Preliminary predicted quantum efficiency for the CCD 273-84 with the sensitivity extended to shorter wavelengths to optimize the spectral region between 180-400 nm.



Our team is in contact with Teledyne Imaging Systems to explore the potential of the newer CMOS detectors as compared to the CCD detectors. One advantage of the CMOS detectors is that they do not suffer from degradation of the charge transfer efficiency over time due to radiation damage, although mitigation strategies exist to minimize this effect in CCD detectors such as those used in HST's WFC3.

## 5. DETAILED NUV/FUV CAMERA DESIGN

### 5.1 Detailed Camera Optical Design<sup>12,13</sup>

An Offner-like relay (similar to that in the MOS) operating over a wavelength range of 115 – 400 nm provides the inputs to a mode select beamsplitter. When this mode select mirror is in the beam, it reflects the light < 400 nm to the FUV channel (and longer light to a beam trap). The FUV channel detector is the 4Kx4K e2v CCD 273-84 (identical to the MOS detector; see section 4.5). When the mode select beamsplitter is moved out of the beam, the light continues to the FUV channel where the 115-175 nm light is directed through spectral band filter(s) to the Micro-Channel Plate detector. The MCP photocathode is CsI with 20 μm “pixels.” The system operates at f/5 and has unit magnification. The field of view is 1045 x 1045 arcsec.

A block diagram of the optical design is shown in **Figure 17**. **Figure 18** shows the current optical design. Trades are also proceeding to look at the science impact of deleting the two filter wheels and their associated cost and simplifying to a single filter in each path.

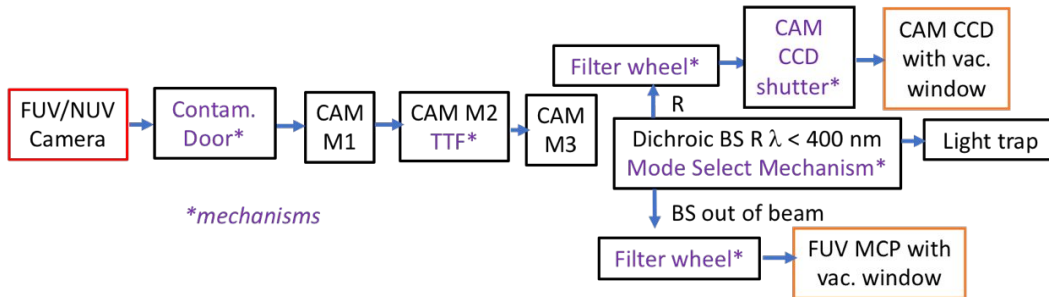


**Figure 17** – FUV/NUV Camera Functional Block Diagram showing the optical path sequence and major functions

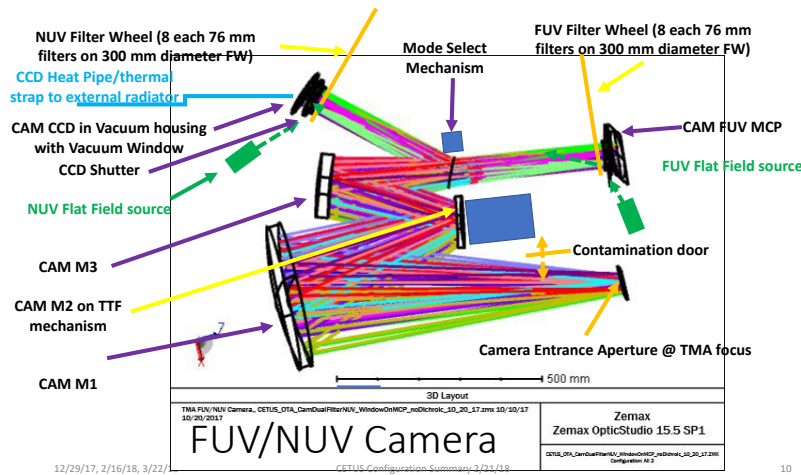


**Figure 18** – The FUV/NUV Camera has 2 separate channels: The FUV channel has a MCP which covers the 115-175 nm and the NUV channel has a CCD which covers the 180-400 nm range. In front of each channel is a filter wheel with filters to define sub-bands of interest.

**Figures 19** and **20** show the performance (spot diagrams) for the FUV and NUV cameras.

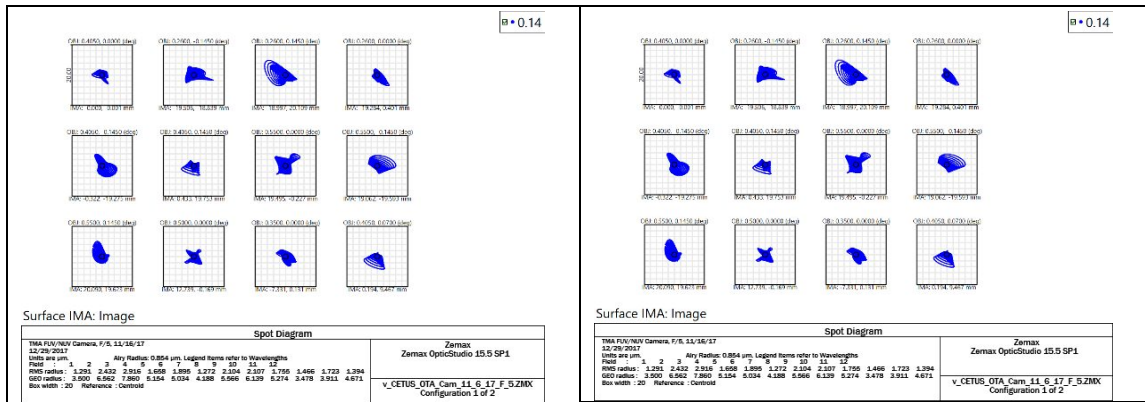


**Figure 19** -- The FUV Camera has a well corrected monochromatic PSF as shown at  $\lambda = 140$  nm. The boxes are  $20 \mu\text{m}$ .

**Figure 20** -- The NUV Camera has a well corrected monochromatic PSF as shown at  $\lambda = 210$  nm. The boxes are  $20 \mu\text{m}$ .

### 5.2 Filters define the science bands of interest

The NUV path is defined by a number of spectral filters that form the sub-bands that will reach the e2v CCD 273-84 detector. These filters are mounted in a filter wheel which can be rotated to 8 different positions (including one used for calibration). The bands being considered are described in **Table 4**.

**Table 4** NUV Camera has a filter wheel with bandpass filters to cover the 180-400 nm spectral range

NUV Filter Wheel position	Filter name	Wc (nm)	FWHM (nm)
1	F202M	202	41
2	LF246W	246	41
3	LF290W	290	41
4	LF334W	334	41
5	LF378W	378	41
6	LF185LP*	UV DYNASIL or equivalent	900
7	LF210N ** (red-shifted Lyman alpha)	210 Wc (z=2)	20

\* NUV 6 (Broad) (185 to  $> 1100$  nm)

\*\*NUV 7 (z2 Ly alpha)

The FUV path also has a filter wheel prior to the detector. However, over the 115nm to 175nm range, it is difficult to fabricate bandpass filters for the desired sub-bands of interest. Instead, long pass filters are used with different starting points and the sub-band data is gleaned from the subtraction of various pairs of filters. **Table 5** lists the longpass filters and their characteristics. The natural spectral transmission of various substrates is essential in forming the desired longpass bands. Sub-bands are analyzed by subtracting the data from two different filter wheel positions. For example, 115-140 nm can be derived by differencing the data from filter position 4 ( $>140$  nm) and filter position 1 ( $>115$  nm) taking into account suitable calibration.

For the FUV channel, the detector is a Micro-channel Plate -- nominally with a Cesium Iodide (CsI) photocathode. A Gallium Nitride photocathode would provide higher quantum efficiency in the FUV and is being considered for a future upgrade should its technology maturation be compatible with the CETUS fabrication timeline.

**Table 5** FUV Camera has a filter wheel with longpass filters to investigate the 115-175 nm spectral range

FUV Filter Wheel position	Filter name	Long Pass	Substrate
1	F115LP	>115 nm	MgF <sub>2</sub>
2	F125LP	> 125 nm	CaF <sub>2</sub>
3	F130LP	>130 nm	SrF <sub>2</sub>
4	F140LP	>140 nm	BaF <sub>2</sub>
5	F142LP	> 142 nm	Al <sub>2</sub> O <sub>3</sub>
6	F150LP	> 150 nm	Quartz crystal
7	F165LP	>165 nm	UV DYNASIL or equivalent

As previously stated, a potential descope being considered is to delete the filter wheels and have a single fixed filter for each channel with some loss of science. These are part of the design-to-cost and potential descope trades.

## 6. SUMMARY/CONCLUSIONS

We have implemented a design-to-cost approach and developed a configuration with adequate tolerances to address all environments. The UV Multi-Object Spectrometer in conjunction with the CETUS 1.5-m aperture will allow the investigation of approximately 100 galaxies at a time to build up an impressive catalog at  $z=1-2$  (over 100,000 targets) over the 5-year lifetime of this part of the mission. Integral to the approach is a large field-of-view, selectable “slit” configurations via a next generation micro-shutter array, and a convex, holographic grating for dispersion. The MOS instrument and companion NUV/FUV Camera would be beneficial to both Probe-class and Large-class missions.

## 7. ACKNOWLEDGEMENTS

John Hagopian (Advanced Nanophotonics, Inc.) has led the technology design and implementation of nanotube light trap approaches. Materion and ZeCoat have provided UV coating designs and data. In addition, further definition of the instrument designs has been supported by NASA through a Probe Study award for CETUS and by GSFC IR&D.

## REFERENCES

- [1] Heap, S., Hull, A., Kendrick, S., et al., “CETUS: An innovative UV probe-class mission concept,” Proc. SPIE 10398, (2017).
- [2] Purves, L., et al., “Mission systems engineering for the Cosmic Evolution Through UV Spectroscopy (CETUS) space telescope concept,” Proc. SPIE 10401, (2017).
- [3] Heap, S., Danchi, W., et al., “The NASA probe-class mission concept, CETUS (Cosmic Evolution Through Ultraviolet Spectroscopy), SPIE 10398, (2017).
- [4] MacKenty, J.W., Stiavelli, M., “A Multi-Object Spectrometer using Micro Mirror Arrays,” Imaging the Universe in Three Dimensions, Proceedings from ASP Conference Vol. 195, p. 443, (2000).
- [5] Hull, A., Heap, S., et al., “The CETUS probe mission concept 1.5m optical telescope assembly: A high A-Omega approach for ultraviolet astrophysics, Proc. SPIE 10699, (2018).

- [6] PATR: Cosmic Origin Program Annual Technology Report, <https://cor.gsfc.nasa.gov/technology/documents/COR2016PATR.pdf>, (October 2016)
- [7] Gunn, J. (2009) <https://arxiv.org/abs/0903.3404>
- [8] Heap, S., et al., "End-to-end simulations and planning of a small space telescopes: Galaxy Evolution Spectroscopic Explorer: a case study," Proc. SPIE Vol. 9911, 991117 (2016).
- [9] Heap, S., et al., "Galaxy evolution spectroscopic explorer: scientific rationale", Proceedings of SPIE Vol. 9905, 990505 (2016).
- [10] Kendrick, S, Woodruff, R., et al., "UV spectroscopy with the CETUS Ultraviolet multi-object spectrometer (MOS)," AAS 140.08, (January 9, 2018).
- [11] MSA: [jwst.nasa.gov/microshutters.html](http://jwst.nasa.gov/microshutters.html)
- [12] Woodruff, R., et al., "Optical design for CETUS: a wide-field 1.5m aperture UV payload being studies for a NASA probe class mission study," Proc. SPIE 10401, (2017).
- [13] Woodruff, R., Danchi, W., et al., "Optical design for CETUS: a wide-field 1.5m aperture UV payload being studies for a NASA probe class mission study," AAS 140.15, (January 9, 2018).
- [14] MacKenty, J., "A near ultraviolet solar-blind telescope design using silicon CCD detectors," SPIE Vol. 990533, (2016).
- [15] Hagopian, J., (2010) <https://www.nasa.gov/topics/technology/features/new-nano.htm>
- [16] <https://www.nasa.gov/content/goddard/super-black-nano-coating-to-be-tested-for-the-first-time-in-space/>  
Hagopian, J., et al., "Multiwalled carbon nanotubes for stray light suppression in space flight instruments," Proc. SPIE 7761, (2010). <http://adsabs.harvard.edu/abs/2010SPIE.7761E..0FH>
- [17] Butler, J., et al., "Initial studies of the bidirectional reflectance distribution function of carbon nanotube structures for stray light control applications," Proc. SPIE 7862, (2010). <http://proceedings.spiedigitallibrary.org/proceeding.aspx?articleid=1348296>
- [18] Li, M, et al., "James Webb Space Telescope microshutter arrays and beyond," *J. Micro/Nanolith. MEMS MOEMS*. 16(2), 025501 (Apr 07, 2017). ; <http://dx.doi.org/10.1117/1.JMM.16.2.025501>
- [19] Development and operation of the microshutter array system | (2008) | Jhabvala | Publications | SPIE